Impaired cell fusion and differentiation in placentae from patients with intrauterine growth restriction correlate with reduced levels of HERV envelope genes

Matthias Ruebner · Pamela L. Strissel · Manuela Langbein · Fabian Fahlbusch · David L. Wachter · Florian Faschingbauer · Matthias W. Beckmann · Reiner Strick

Abstract One leading cause of perinatal morbidity and mortality is intrauterine growth restriction (IUGR). Several causes for IUGR have been proposed involving cytotrophoblast dysfunction. Envelope genes of the human endogenous retrovirus (HERV)-W (Syncytin-1), -FRD (Syncytin-2), and -P(b) have fusogenic properties, whereas envelope genes of HERV-R, -V1, and -V2 have putative placental functions. All six HERV envelope genes and three known cellular receptors were analyzed for expression in human control and IUGR placentae (n=38) and in cultured cytotrophoblasts from control and IUGR (n=8) placentae. All envelope genes demonstrated downregulation in IUGR compared to control placentae tissues, which were confirmed with cultured cytotrophoblasts. Examination of the Syncytin-1 and Syncytin-2 receptors ASCT-1/-2 and MFSD2 showed that MFSD2 was significantly expressed lower in IUGR than in control placentae and cytotrophoblasts. A reduction of Syncytin-1 protein expression was confirmed for IUGR placentae with immunoblotting and paraffin tissue sections. Embedded placental IUGR tissues showed an overall disorganized syncytiotrophoblast layer with fewer nuclei. Cytotrophoblasts from IUGR placentae demonstrated a lower cell fusion index and nuclei per syncytiotrophoblast in vitro. Fusogenic and non-fusogenic envelope genes are dysregulated in IUGR placentae and may contribute to the etiology of growth restriction in utero.

Keywords Placentogenesis · Cell fusion · HERV · IUGR · Syncytin-1 · Trophoblast

Electronic supplementary material The online version of this article (doi:10.1007/s00109-010-0656-8) contains supplementary material, which is available to authorized users.

M. Ruebner · P. L. Strissel · M. Langbein · F. Faschingbauer · M. W. Beckmann · R. Strick (✉)
Department of Gynaecology and Obstetrics, Laboratory for Molecular Medicine, University-Clinic Erlangen, Universitaetsstr. 21-23,
91054 Erlangen, Germany
e-mail: Reiner.Strick@uk-erlangen.de

F. Fahlbusch
Department of Paediatrics and Adolescent Medicine, University-Clinic Erlangen,
91054 Erlangen, Germany

D. L. Wachter
Institute for Pathology, University-Clinic Erlangen,
91054 Erlangen, Germany

Introduction

The human placenta represents a temporary organ where cell fusions or syncytia are found. During days 6–11 at the time of human blastocyst implantation, villous cytotrophoblasts (CT) fuse to a multinuclear syncytiotrophoblast (SCT), which is followed by fusion of villous CT into the established SCT for enlargement and maintenance [1]. It is known that low oxygen levels play a role during placentogenesis of the first trimester. However, after the removal of the extravillous trophoblast plugs, which block the spiral arteries, the SCT becomes in direct contact with the normal oxygenated blood from the mother [2, 3]. This specialized SCT functions as the primary feto-maternal interface or barrier essential for nutrient, gas, and waste exchange [4]. Intrauterine growth restriction (IUGR) occurs with an incidence from 4% to 7% live births and remains one major perinatal problem, causing morbidity and mortality of mother and fetus [5, 6]. It is widely accepted that next to infections, maternal diseases, and chromosomal abnormalities, a lack of nutrients and oxygen could lead to IUGR, as

well as impaired fetal-placental angiogenesis [7, 8]. Previously, the measurement of chorionic villi surface areas demonstrated lower values for IUGR (~8.2 m^2) compared to control placentae (~10 m^2), resulting in a smaller interface between maternal and fetal tissues [9]. In addition, IUGR placentae showed an abnormal cellular development of trophoblasts, like lower amounts of CT and more apoptotic SCT [9–11].

Human endogenous retroviruses (HERVs) comprise approximately 8% of the human genome. HERV sequences have homologies to known retroviruses and originated from infections of germ cell lines followed by recombinations, insertions, mutations, and deletions within the host DNA. Over 30,000 HERV elements have been grouped into more than 80 families according to sequence homologies [12, 13]. The envelope (env) gene of HERV-W (chromosome 7q21.2), called Syncytin-1, was the first to be recognized as essential for mediating trophoblast cell fusion events [14, 15]. Interestingly, using cell culture with various oxygen levels from 1% to 20%, Syncytin-1 gene expression can be regulated [16–20].

Furthermore, the Na^+-dependent transporters for neutral amino acids ASCT-2 (SLC1A5) and ASCT-1 (SLC1A4) were also demonstrated as essential for cell fusions, probably by serving as receptors for Syncytin-1 [21]. Recently, two more HERV env genes capable of inducing cell fusions have been identified: HERV-FRD or Syncytin-2 on chromosome 6p24.1 and HERV-P(b) at 14q32.12, which we presently propose to name Syncytin-3 due to its cell fusion ability (Fig. 1a, Supplemental Table 1a in ESM 1).

In addition to placenta, syncytial cells were also found in human endometrial and breast carcinomas, with Syncytin-1 overexpressed [22, 23]. Furthermore, a role for Syncytin-1 mediating fusions was demonstrated for both human endometrial and breast carcinoma cells in vitro. Cancer cell fusions in vitro and in vivo have also been demonstrated to occur between different cell types, e.g., tumor cells and bone marrow-derived cells where these fusions have been implicated in metastasis [24]. Syncytin-2 was detected in villous CT and shown to induce cell fusions using an in vitro cell culture assay with human cancer cells similar to Syncytin-1 [25, 26]. A placenta-specific receptor for Syncytin-2 was identified as a major facilitator superfamily domain containing 2 (MFSD2) gene, which belongs to the large family of putative carbohydrate transporters. MFSD2 was specifically expressed in human placentae and mainly in SCT [27]. The more widely expressed Syncytin-3 was also found fusogenic in cell culture, even with other species than humans [28]. A receptor for Syncytin-3 has not been identified to date.

In addition to the fusogenic Syncytin-1,-2, and -3 env genes, other HERV env genes were found expressed in human placentae. For example, HERV-R or ERV3 (endogenous retroviral sequence 3) mRNAs are abundant in human placental chorion [29] but also expressed in normal and malignant tissues [30]. Although the evolutionary conservation of the envERV3 implies a favorable function, the loss of envERV3 in new world primates and gorillas and the detection of a stop-codon polymorphism in humans leading to a truncated env protein have been proposed against an essential role for survival and reproduction [31, 32]. Recently, HERV-V1 and HERV-V2 along with their respective env genes envV1 and envV2 were located on chromosome 19q13.41 with only ~34 kb between both HERVs [33]. Both envV1 and envV2 were found highly identical with variations only at the C terminus. Recent expression analysis of envV1/V2 demonstrated exclusive expression in the placenta [28, 33].

The aim of this study was to determine if different expression levels of the three fusogenic Syncytin genes and the receptors ASCT-1, -2, and MFSD2, as well as envERV3, envV1, and envV2, contribute to the placental dysfunction in IUGR. In addition, isolated and cultivated CT from control and IUGR placentae were used to determine (1) if the same HERV env expression levels compared to primary placentas and (2) if dysregulated cell fusion occurred using normal cell culture conditions.

Materials and methods

Patient and tissue collective

The diagnosis of IUGR was based on elevated pulsatility index (PI) in the uterine arteries and/or early diastolic notches in both uterine arteries, elevated PI in umbilical arteries, elevated head/abdomen ratio, reduced amniotic fluid index and longitudinal measurements of reduced growth of the fetal abdominal circumference (<5 mm/week), and cross-sectional records of the estimated fetal weight below the tenth percentile [34]. With the approval of the Ethics Committee at the University of Erlangen-Nuremberg, a total of 46 human placentae were obtained from 23 controls and 23 patients solely with IUGR and no other disease, like cancer, diabetes, preeclampsia, or HELLP-syndrome, after elective Cesarean section. The clinical data of the control cohort and patients with IUGR are presented in Table 1. A biopsy was obtained near the cord from every placenta. Placental tissues for RNA and protein analyses (19 tissues from control and 19 from IUGR placentae) were snap frozen in liquid nitrogen and stored at −80°C until further use. In addition, from the 19 control and 19 IUGR placentas, six probes of three control and three IUGR placentae were formalin fixed for immunohistochemistry analyses (see below). Besides the 19 control and 19 IUGR placentae, four additional control

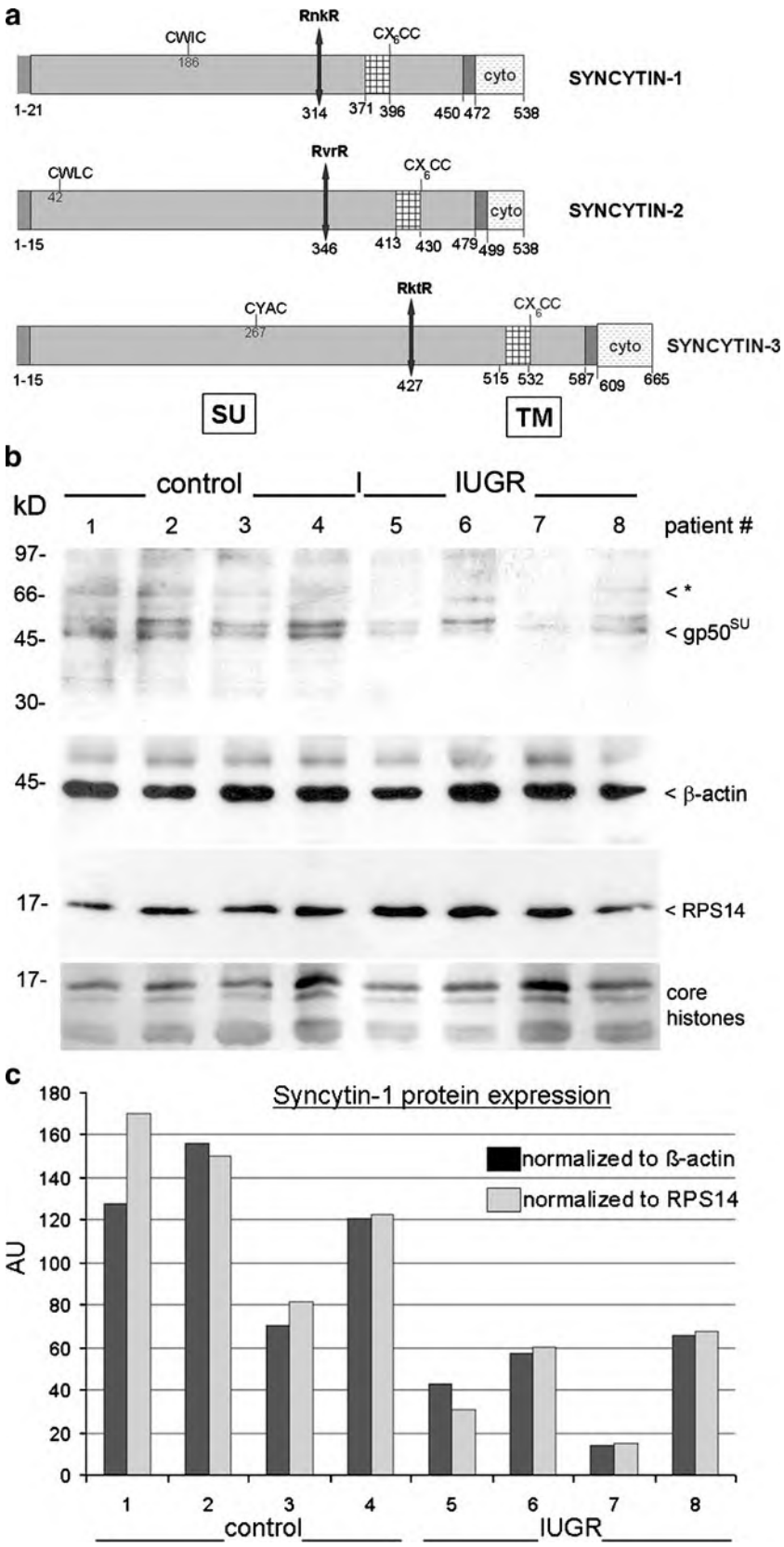

Fig. 1 **a** Comparison of Syncytin-1, -2, and -3 with its SU and TM units divided by the putative protease site recognized by the consensus site RXR/KR or RR/KXR (*X* represents any amino acid). *Numbers* represent amino acid positions; with the N-terminal signal peptide, the immunosuppressive (*squares*), the transmembrane (*dark*), and cytoplasmatic domain (*dashed*). In addition, the putative disulfide sites (*CW/YXC*, CX_6CC) are indicated. **b** Fifteen micrograms of cell lysates from four control and four IUGR placentae were analyzed on a 7.5–12.5% or 7.5–15% gradient SDS-PAGE and hybridized with a SU-specific Syncytin-1 ($gp50^{SU}$), β-actin, and RPS14 antibodies. * represents the Syncytin-1 precursor (gPr66-env) proteins. In addition, the membrane was stained with amido black to detect core histones for equal protein loading and transfer. Left numbers indicate the sizes in kilo-Dalton (*kD*). **c** Syncytin-1 (*gp50*) expression of control and IUGR placentae of immunoblots in Fig. 1b was quantified after normalization against core histones and either β-actin (*black*) or RPS14 (*grey*). Note the similar band intensities between β-actin and RPS14

Table 1 Clinical characteristics

All placentae + trophoblasts		Birth weight (g)	Placenta weight (g)	Age mother (year)	Week of gestation (weeks and week + day)		Gravidity	Parity	Glucose child (mg/dl)	Glucose mother (mg/dl)
n=23	Control	2,800.05	567.27	30.29	37.15	37+1	2.00	0.47	86.33	86.13
	SEM	±226.12	±26.35	±1.44	±0.73	±0+5	±0.27	±0.17	±8.51	±5.71
n=23	IUGR	1,952.63	363.33	29.85	36.39	36+3	1.79	0.68	57.55	86.23
	SEM	±138.27	±73.60	±1.43	±0.69	±0+5	±0.22	±0.21	±5.33	±5.29
	P	0.000369**	0.01034*	0.829984	0.2229610		0.616308	0.616308	0.015897*	0.971773

*$P<0.05$ (significant)

**$P<0.005$ (highly significant)

and four IUGR placentae were used for CT fractionations (see below); thus, the total number of control placentae was 23 and of IUGR placentae was 23 (Table 1).

RNA extraction and cDNA synthesis

Total RNA was extracted from 50 to 100 mg of frozen placental tissues according to Strick et al. and Langbein et al. [23, 35]. For expression analysis, RNA was pre-treated with DNase I (Sigma-Aldrich, Germany), and cDNA was generated with the High Capacity cDNA Kit (Applied Biosystems (ABI), Germany) in a thermal cycler (ABI2720) for 2 h at 37°C.

Semi and absolute quantitative real-time PCR

Supplemental Table 1a in ESM 1 shows specific primers of the env genes Syncytin-1, -2, and -3, envERV3, envV1, and envV2 used for cloning PCR fragments into TopoTA vectors (Invitrogen). The DNA of the cloned env genes with known copy numbers was used as an external standard to generate a standard curve with the cycle threshold (C_T) value against the log of amount of standard (ABI7300). Quantitative real-time PCR (qPCR) with specific primers were then used to quantitate all env genes of placentae and trophoblasts (40 ng cDNA/well) with SYBR-green technology (Supplemental Table 1a in ESM 1). Amplification of 18S-rRNA (TF 5′ GCAATTATTCCCCATGAACG and BR 5′ GGCCTCACTAAACCATCCAA) and β-actin (TF 5′ TCACCATTGGCAATGAGCGG and 5′ BR: GATGTC CACGTCACACTT CAT) was used for normalization of the different samples using each 1 ng cDNA/well. The normalization with 18S-rRNA (C_T=12.7) and β-actin (C_T= 23.3) showed the same results in env gene expression. Importantly, a similar PCR efficiency (over 97%) between all env genes was needed in order for comparison. Similar standard curves of all env genes were obtained for the SYBR-green based qPCR with the following slopes and calculations (Supplemental Table 1b in ESM 1). The analysis of the Syncytin-1 and -2 receptors was performed using semiquantitative TaqMan assays (Applied Biosystems) for ASCT-1 (exon 7-8), ASCT-2 (exon 1-2), and MFSD2 (exon 13-14) using placentae and trophoblasts with 50 ng cDNA/well. Co-amplification of 18S-rRNA (Applied Biosystems) and one control cDNA as internal control were used for a standard curve in semi-quantitation analysis.

Immunoblot analysis

Proteins were isolated from frozen placenta tissues according to Strick et al. [23]. Fifteen micrograms of cell lysates were resolved on a 7.5–12.5% or 7.5–15% acrylamide gradient SDS-gel, transferred to a NC membrane using a CAPS-transfer buffer according to Strick et al. and Langbein et al. [23, 35]. In order to verify overall protein content per placenta lysate, membranes were stained after transfer with amido black (Sigma-Aldrich). The membranes were incubated with a Syncytin-1 SU-specific monoclonal antibody (clone 4F10; 1:1,000; Abnova, Tebu-Bio, Offenbach, Germany). A secondary peroxidase-labeled monoclonal antibody was used for detection (1:1,000; Sigma-Aldrich). Blots were stripped and incubated with β-actin monoclonal antibody (1:1,000; Cell Signaling, Frankfurt, Germany), or blots were incubated with RPS14 polyclonal antibody (1:1,000; Abcam, Cambridge, UK) for normalization. RPS14 is essential for the correct processing of 20S- to 18S-rRNA and therefore can be used for a direct comparison of real-time PCR (normalization against 18S-rRNA) and immunoblots. Normalizations of protein band intensities were first done against core histones and then either against β-actin or RPS14 using ImageJ®.

Fractionation and cultivation of cytotrophoblasts

Human CT was isolated using the well-established trypsin-DNase-Dispase/Percoll method [20, 35–37] from four independent control and four IUGR placentae and cryopreserved in liquid nitrogen. We analyzed the specific Percoll gradient cell fraction (1.048 to 1.062 g/ml density) with the following results: (1) CT viability was routinely >85%

using trypan blue exclusion; (2) using multiple FACS (FACSCalibur, BD Biosciences) analyses of each of the four control and four IUGR fractionated CT met specific requirements. For example, we determined that 10–13.3% of the fractions were HLA-A,B,C+(mononuclear blood cells, fibroblasts, and other rare cell types) and 86.6–90% HLA-A,B,C negative (Suppl. Fig. 1a in ESM 1). In addition, fractionated cells were 95.5–97.6% CK7+ (many epithelial cells) and 2.4–4.5% CD45+ (mononuclear blood cells) [CK7/PE (clone 5F282), Santa Cruz Bio., Heidelberg, Germany (1:20); HLA-A,B,C/PE (cloneW6/32), Biolegend, Uithoorn, Netherlands (1:10); CD45/FITC, Miltenyi Biotec, Berg. Gladbach, Germany (1:10)] (Suppl. Fig. 1b in ESM 1). Therefore, 86.6–90% of the fractionated cells were trophoblastic cells and 10–13.3% non-trophoblastic. A further FACS analysis using propidium iodide (Sigma; 50 μg/ml), specific for DNA content, resulted in 6.8–8.5% multinucleated fractured syncytial fragments. On the other hand, an estimation of fractured syncytial fragments with one or two nuclei could not be performed (Supplemental Fig. 1c in ESM 1). However, all fractured syncytial cellular fragments, non-adherent cells, and debris were removed initially after 4 h and then every 24 h with a media change [38]; (3) following the seeding of 300,000 viable cells per square centimeter (trypan blue negative) in Dulbecco's Modified Eagle's Medium supplemented with 10% fetal calf serum, 20 mM Hepes, 2 mM L-glutamine, penicillin/streptomycin (100 U/ml, 100 μg/ml), and non-essential amino acids in a humidified 5% CO_2 environment at 37°C, CT were cultivated for 3 days. After 3 days of culturing, CT were routinely assessed by immunohistochemistry for CK7 and Vimentin (non-epithelial cells) [35]. In general control and IUGR CT were approximately 95% CK7+ and up to 5% Vimentin+.

Assessment of fused cells by May-Gruenwald-Giemsa and membrane staining

CT cultures at day 3 were analyzed microscopically for cell fusions using two methodologies: (1) May-Gruenwald-Giemsa staining (Sigma-Aldrich) and (2) wheat germ agglutinin (Alexa 594) plasma membrane stain along with the nuclear stain Hoechst 33342 (Molecular Probes, Karlsruhe, Germany) according to Strick et al. and Langbein et al. [23, 35]. Eight different visual fields from each CT culture from control (n=4) and IUGR placentae (n=4) were analyzed to determine the fusion index (FI) and the number of nuclei/SCT by two independent researchers. The FI was calculated according to the formula $FI=[(N-S)/T]\times 100$, where N represented the amount of nuclei in SCT, S the quantity of SCT, and T the total nuclei. Analysis was performed by microscopy (Zeiss, IM35) with different objective lenses (10× Neofluor 10/0.30 and 20× LWD 160/0-2). Images were acquired with a digital camera (Canon EOS400D) under the same camera adjustments (aperture and shutter speed) for control and IUGR and were processed identically with computer software (Photoshop CS3). The measurement of total human chorionic gonadotropin (β-hCG) as a biochemical differentiation marker was performed with an Immulite2000 (DPC) [39, 40].

Hematoxylin/eosin staining of paraffin-embedded placentae

Three control and three IUGR placentae probes were fixed in 10% formalin for 1 h, washed several times with ethanol (70–100%) for 5.5 h and xylol (2.5 h), and embedded into paraffin (2 h). Hematoxylin/eosin staining was performed by automation (Gemini, Shandon Varistain) following deparaffinization with xylol for 10 min, washed with ethanol and water, and then stained with hematoxylin gill #3 (3 min) and eosin (20 s). Eighteen microscopic regions with two to three villi (more than 36 villi per placenta) were analyzed as nuclei per millimeter. The calculation of nuclei per SCT in longitudinal cuts of anchoring and floating villi of control and IUGR placentae was performed for a total of 108 villi for control and 108 villi for IUGR.

Fast Red–hematoxylin staining (Zytomed Systems, Berlin, Germany)

Placentae probes were deparaffinized with xylol and rehydrated to 70% ethanol, washed in 0.1 M Tris–HCl pH 8.6, and pre-treated with Target Retrieval Solution (pH 9; Dako, Hamburg, Germany). Probes were blocked in Blocking Solution (Reagent I) for 5 min and incubated overnight at room temperature (RT) with 1:100 diluted Syncytin-1 SU-specific polyclonal antibody (Biozol, Germany). After washes with Tris–HCl pH 8.6, probes were blocked with PostBlock (Reagent II) for 30 min at RT, treated with two drops of Brij®, and incubated with AP-Polymer (Reagent III) for 30 min at RT. Probes were stained with filtered Fast Red staining solution (2 mg Naphtol-AS-MX-Phosphat, 0.2 ml N,N-dimethylformamide, 9.8 ml 0.1 M Tris–HCl pH 8.6, 10 μl 1 M Levamisole for inhibition of endogenous phosphatase activity, 10 mg Fast Red) for 20 min at RT (Zytomed Systems, Berlin, Germany). Probes were washed briefly under floating water and counterstained with a Hämalaun Mayer solution for 10 s. As a negative control, the same procedure was done without the primary antibody Syncytin-1. The fluorescent analyses were performed with filters at 670 nm. Probe analyses and image acquisition were performed as described in the May-Gruenwald-Giemsa and fluorescent membrane staining protocols.

Statistical analysis

The nonparametric Mann–Whitney test for independent samples was performed using SPSS 16.0.2. (SPSS, Inc.). For all tests, a $P<0.05$ was considered as statistically significant. For each mean value, a standard error of the mean was calculated using SPSS 16.0.2.

Results

As expected the birth and placenta weight of IUGR newborns showed a significant difference as compared to the control cohort. Both cohorts had similar ages, gravidity, and parity; however, the glucose concentration of IUGR newborns was significantly lower (Table 1). Comparing the absolute expression of env genes by qPCR demonstrated that Syncytin-1 was expressed the highest in control placentae in the following order: Syncytin-1 > envERV3 > Syncytin-2 > envV2 > envV1 > Syncytin-3. Importantly, the expression levels were similar after normalization for 18S-rRNA (Table 2 and Fig. 2) and β-actin (data not shown).

Regarding only the fusogenic env genes (Syncytin-1, -2, -3), Syncytin-1 expression was 10- and 145-fold higher than Syncytin-2 and Syncytin-3 levels, respectively (Fig. 2, Table 2). In IUGR placentae, not only the order of expression was changed for envV1 and envV2 compared to control primary tissues (Syncytin-1 > envERV3 > Syncytin-2 > envV1 > envV2 > Syncytin-3), but a significant lower expression for Syncytin-1 (2.1-fold), Syncytin-2 (4.7-fold), envV1 (twofold), and envV2 (six-fold) was found (Fig. 2, Table 2). In general, all three fusogenic env genes together were 2.2-fold expressed lower in IUGR placentae (686.84 to 308.53 molecules/ng, $P=0.000036$) and all six env genes 1.7-fold lower (957.75 to 560.17 molecules/ng, $P=0.012959$) compared to control placentae (Table 2). Furthermore, a lowered protein expression of Syncytin-1 in IUGR placental tissue ($n=4$) compared to control placenta ($n=4$) was confirmed with immunoblot analysis using a Syncytin-1 SU-specific monoclonal antibody (Fig. 1b). Control placentae showed more processed Syncytin-1 SU-protein (gp50) and the Syncytin-1 precursor protein (gPr66) than the IUGR placenta extracts. Among all four IUGR placentae compared to four controls, Syncytin-1 protein (SU=gp50) levels following normalization against core histones and β-actin resulted in 62.1% less protein; and against core histones and RPS14 66.8% less protein (averaged normalized values; Fig. 1b, c).

Fractionated CT from control ($n=4$) and IUGR placentae ($n=4$) were cultured for 3 days and then analyzed for HERV env expression. Control placental CT demonstrated

Table 2 Gene expression of all six env in control and IUGR placentae and isolated trophoblasts

		Syncytin-1	Syncytin-2	Syncytin-3	Sum of Syncytin-1+2+3	envErv3	envV1	envV2	Sum of all env
Placenta tissues									
$n=19$	Control	623.84	58.53	4.37	686.84	365.32	14.59	24.63	957.75
	SEM	±65.46	±17.86	±0.88	±74.44	±70.87	±3.85	±13.46	±114.74
$n=19$	IUGR	292.68	12.32	3.42	308.53	269.32	7.46	4.05	560.17
	SEM	±49.54	±4.05	±1.14	±53.20	±58.99	±2.92	±1.47	±89.40
	P	0.000283**	0.000188**	0.310719	0.000036**	0.212005	0.002476**	0.02527*	0.012959*
Isolated trophoblasts									
$n=4$	Control	2,827.00	29.00	3.50	2,859.25	550.00	414.13	230.48	4,053.85
	SEM	±676.81	±11.72	±0.64	±687.03	±184.02	±199.70	±85.55	±1,019.62
$n=4$	IUGR	219.50	1.25	2.25	223.00	72.75	14.90	7.98	318.55
	SEM	±51.21	±0.25	±1.03	±50.81	±21.51	±6.65	±3.13	±45.60
	P	0.020921*	0.017249*	0.374857	0.020921*	0.020921*	0.020921*	0.020921*	0.020921*

All values are in molecules per nanogram total cDNA

*$P<0.05$ (significant)

**$P<0.005$ (highly significant)

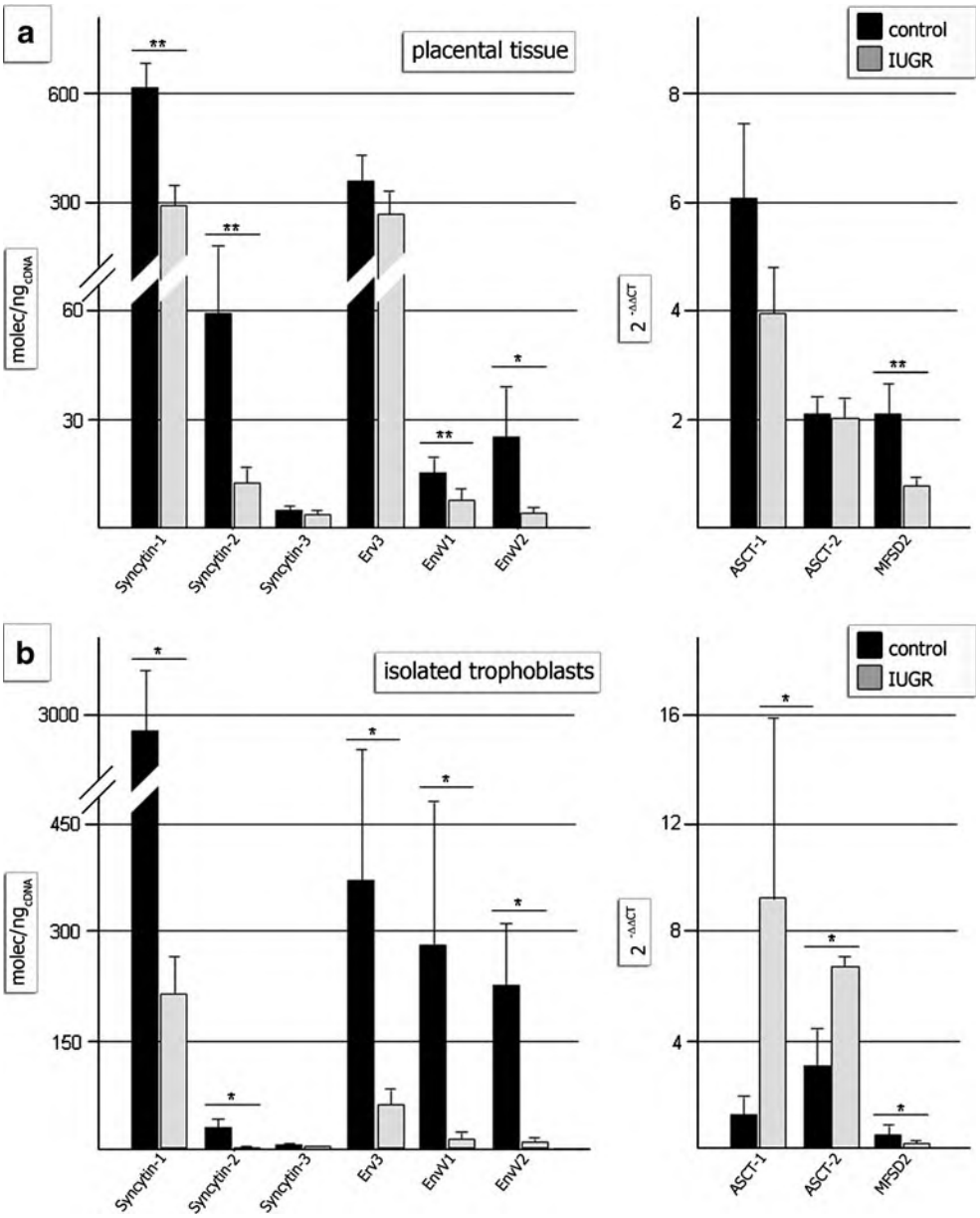

Fig. 2 *Bar graphs* representing data from Tables 2 and 3. Shown are absolute molecules per nanogram cDNA calculated by qPCR for the six different HERV env genes and three receptors using semiquantitative real time PCR. **a** Placental tissues from control and IUGR; **b** fractionated trophoblasts from control and IUGR placentae analyzed at day 3 of culturing. * Significant, ** highly significant differences

that Syncytin-1 and envERV3 were expressed the highest among all env genes in the following hierarchy: Syncytin-1 > envErv3 > envV1 > envV2 > Syncytin-2 > Syncytin-3 (Table 2, Fig. 2 with 18S-rRNA and β-actin; data not shown). Comparing expression levels to primary control tissues showed differences. For example, Syncytin-1 and envERV expression was 4.5- and 1.5-fold higher in cultured control CT compared to control placentae, respectively (Table 2). In addition, control CT had higher envV1 (28.5-fold) and envV2 (9.6-fold) levels compared to control placentae. Syncytin-2 and -3 CT expression values were comparable to primary control tissues (Table 2, Fig. 2).

Although the hierarchy of env gene expression in isolated CT from IUGR placentae was almost similar to CT from control placentae (Syncytin-1 > envErv3 > envV1 > envV2 > Syncytin-3 > Syncytin-2), env expression values were lower; for example, Syncytin-1 and envErv3 were 12.88- and 7.56-fold lower compared to control CT, respectively. Except for Syncytin-3, the env expression differences between control and IUGR fractionated CT were similar but more dramatically decreased than between control and IUGR primary tissues. (Table 2). Syncytin-1, -2, -3 together were 12.8-fold lower expressed in IUGR CT (2,859.25 to 223.00 molecules/ng, $P=0.020921$) and all six env genes 12.7-fold lower (4,053.85 to 318.55 molecules/ng, $P=0.020921$) compared to control CT (Table 2).

Analyzing the ratios of the Syncytin-1 receptors ASCT-1 and -2 were not significantly different between the control and IUGR placentae; however, the Syncytin-2 receptor MFSD2 was significantly 2.7-fold downregulated in IUGR

placentae (Table 3, Fig. 2). In contrast, in isolated IUGR CT cultivated for 3 days, a significant higher expression level was found for ASCT-1 (9.8-fold) and ASCT-2 (2.2-fold) than in control CT (Table 3). Similar to primary placentae, the Syncytin-2 receptor MFSD2 demonstrated a significant reduction of expression in IUGR CT compared to control CT (Table 3, Fig. 2). In addition, β-hCG levels as a marker for CT differentiation were determined from each CT culture supernatant after 3 days and revealed 80.2-fold higher concentrations for control CT when compared to IUGR CT (Fig. 3b). Comparing the mean fusion index of isolated CT from control placentae (n=4) and IUGR placentae (n=4) showed a significant ~20% lower fusion level in IUGR CT (83.16% to 63.24%). A simultaneous analysis of the mean amount of nuclei per SCT after 3-day cultures demonstrated a non-significant higher nuclei number for isolated CT from control placentae (n=4; 10.7 nuclei per SCT) compared to IUGR placentae (n=4; 8.55 nuclei per SCT; Fig. 3).

A comparative analysis of paraffin-embedded placentae from control and IUGR patients revealed similar results to isolated and cultivated CT concerning the SCT formation and nuclei/SCT amount. Nuclei of SCT in anchoring and floating villi from IUGR placentae had a more disorganized appearance than control placentae, where nuclei looked more like a "string of beads" (Fig. 4). A calculation of nuclei per SCT in 36 villi total per placentae revealed that IUGR placentae (n=3) had significantly 25.6% less nuclei present than control placentae (n=3; control: 51.5±1.66 nuclei/mm and IUGR 38.3±1.16 nuclei/mm; P= 0.00000003; Fig. 4). A further analysis of deparaffinized probes from control and IUGR placentae for Syncytin-1 expression and villi characteristics was performed with a Syncytin-1 polyclonal antibody (SU-specific) and Fast Red–hematoxylin (Fig. 5). A comparison of Syncytin-1 expression revealed an overall stronger signal in the control placentae than IUGR placentae, supporting our immunoblot Syncytin-1 analysis (Fig. 1b). Syncytin-1 showed an intense membrane staining at the villi and appeared more concentrated at the apical site of the SCT.

Discussion

Gene expression analysis comparing six env genes in control term placentae demonstrated Syncytin-1 with the highest and Syncytin-3 with the lowest expression levels (Table 2). Syncytin-1, -2, and -3 genes were previously demonstrated to induce cell fusions in vitro [15, 25, 28, 41]. Although similar in function, this study demonstrated great variations between their expression levels in primary placental tissues where Syncytin-1 was tenfold higher expressed than Syncytin-2 and 145-fold higher than Syncytin-3. Another study also found a lower expression of Syncytin-2 compared to Syncytin-1 in human placenta, but only with a ~2.7-fold difference [42]. The differences in expression of the three fusing env genes after 3-day cultivation of control CT were more dramatic than in control placental tissue where Syncytin-1 was 97.5-fold higher expressed than Syncytin-2 and 807.7-fold more than Syncytin-3, which could be explained by fractionation of CT.

As shown with Syncytin-1 transfections, Syncytin-1 antibodies, and specific siRNAs, Syncytin-1 is considered the cardinal gene for cell fusions [15, 22, 23, 43, 44]. Syncytin-1 was detected in villous and extravillous CT and SCT, but Syncytin-2 was only detected in villous CT by immunohistochemistry, supporting that Syncytin-2 plays a possible role in the initial part of CT fusion [26, 41]. The different expression pattern of Syncytin-2, but also of its receptor MFSD2, which is specifically expressed in trophoblasts supports their role in the CT to SCT fusion or with the in-fusion process maintaining the organization of the syncytiotrophoblast [1, 27]. Syncytin-3 was also

Table 3 Gene expression of the cellular receptors of Syncytin-1 and -2

		ASCT-1 ($2^{-\Delta\Delta CT}$)	ASCT-2 ($2^{-\Delta\Delta CT}$)	MFSD2 ($2^{-\Delta\Delta CT}$)
Placenta tissues				
n=19	Control	6.02	2.06	2.05
	SEM	±1.34	±0.28	±0.54
(n=19)	IUGR	3.94	2.01	0.76
	SEM	±0.84	±0.34	±0.12
	P	0.310719	0.686145	0.002222**
Isolated trophoblasts				
n=4	Control	1.15	3.00	0.67
	SEM	±0.65	±1.25	±0.33
n=4	IUGR	11.23	6.71	0.18
	SEM	±6.63	±0.29	±0.08
	P	0.020921*	0.043308*	0.043308*

*P<0.05 (significant)

**P<0.005 (highly significant)

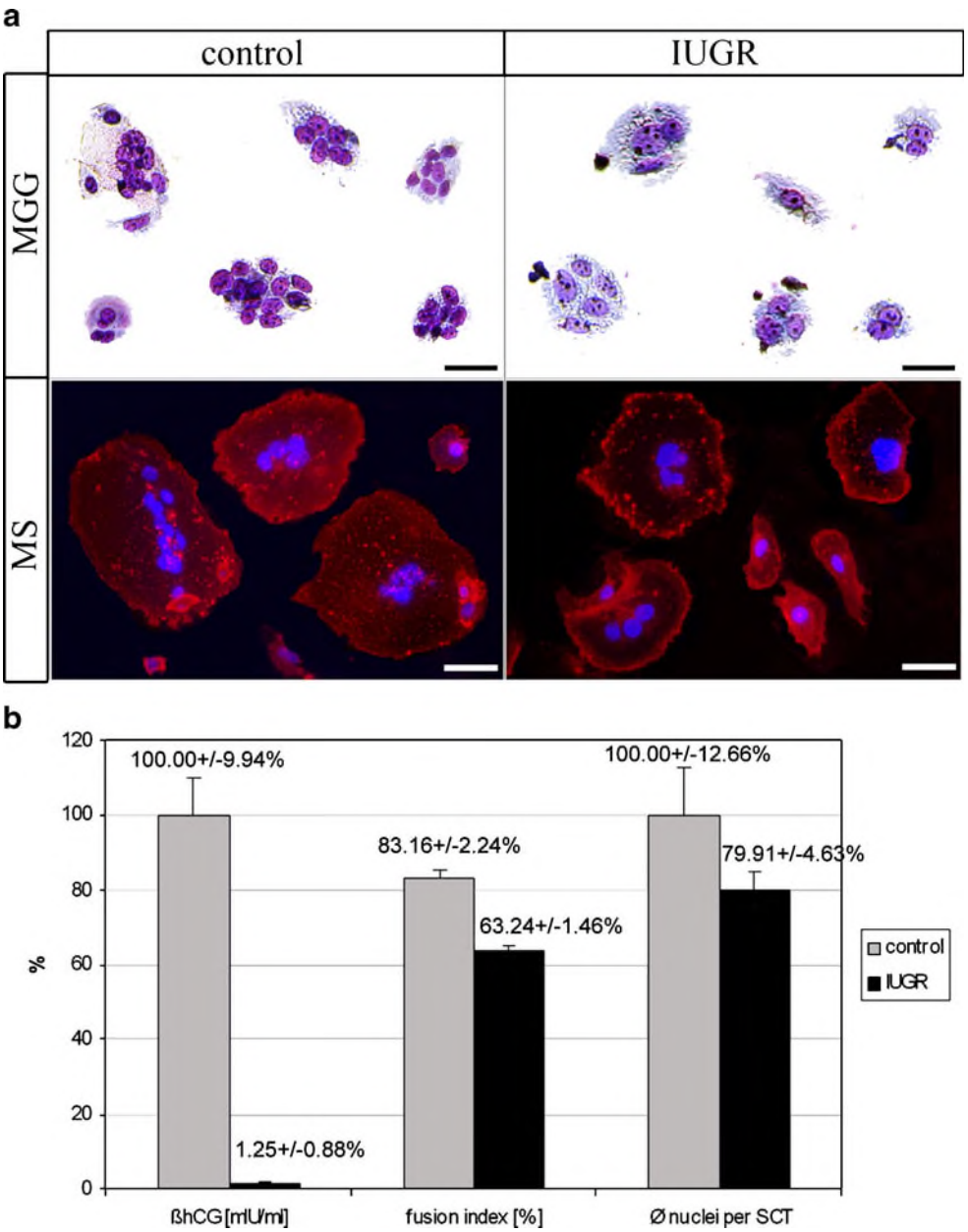

Fig. 3 **a** Fractionated CT from control and IUGR placentae were cultivated for 3 days and analyzed for spontaneous cell–cell fusion (SCT) by May-Grunwald-Giemsa (*MGG*) staining and microscopy. Note the different amounts of nuclei per SCT. In addition, CT were stained with a specific cell membrane stain (*MS*) of wheat germ agglutinin with Alexa 594 and nuclear Hoechst 33342 stain. *Bars* represent 50 μm. **b** Histogram of β-hCG, fusion index, and mean number nuclei per SCT in % of control trophoblasts (n=4) and IUGR trophoblasts (n=4). Absolute values for β-hCG were control, 4,077.50±405.52 mIU/ml SEM; IUGR 50.86±36.18 mIU/ml SEM (P=0.02092); and for mean nuclei per SCT control 10.7±1.35 SEM; IUGR 8.55±0.49 SEM (P=0.11384). The P value for the fusion index was P=0.001566

detected in other tissues than placentae, and to date, it is unclear which role Syncytin-3 plays in CT fusions and which placental cells express Syncytin-3. However, in vitro experiments showed that villous CT and possibly SCT express Syncytin-3 [28]. All of the above support that the different expression levels of the three Syncytin genes points to distinct functions during the cell fusion process in time, cell type, or localization of the placenta.

In previous studies, Syncytin-1 expression was found decreased in placentae from preeclampsia and HELLP patients associated with IUGR [17, 35, 45]. In this investigation, we determined significantly lower Syncytin-1 levels at the RNA and protein levels solely in IUGR placentae compared to control placentae (Table 2 and Figs. 1, 2, and 5). Importantly, Syncytin-2 expression levels were also decreased in IUGR placentae. Calculating the absolute number of all three fusogenic Syncytins, a significantly 2.2- or 12.8-fold more molecules of Syncytin-1/-2/-3 per nanogram of total cDNA were found in control placentae compared to IUGR placentae and control CT compared to IUGR CT, respectively (Table 2). These differences in fusogenic Syncytins could be linked to IUGR etiology. For example, lower expression of Syncytin-1 and -2 in IUGR placentae and CT could be the cause for the significantly lower cell fusion index in IUGR CT (Fig. 3). Although substantially reduced levels of Syncytin-1 and -2 in IUGR CT were detected, we only observed a ~20% decrease of the IUGR CT cell fusion index and nuclei/SCT along with an equivalent 25.6% lower nuclei amount in paraffin-embedded IUGR placentae (Figs. 3, 4).

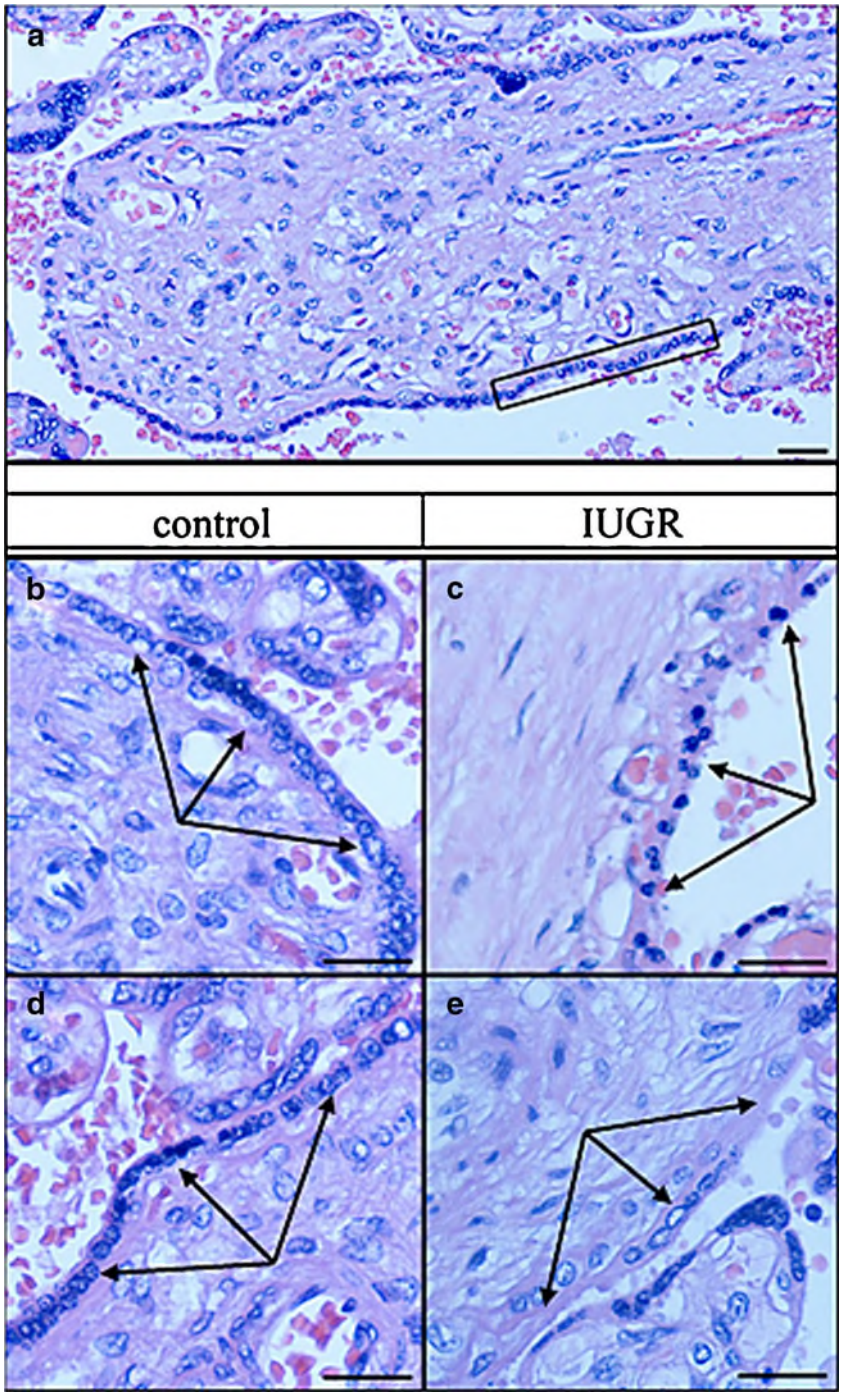

Fig. 4 Paraffin-embedded placentae from control and IUGR patients were stained with hematoxylin and eosin. **a** Example of villi of a control placenta with the SCT layer. *Rectangle* that displays 500 μm in length was used for counting SCT nuclei. **b**, **d** Zoom of control SCT and **c**, **e** zoom of IUGR SCT. Note the different nuclei organization and quantity (*arrows*). *Bars* represent 100 μm

In addition, the more disorganized appearance of the SCT layer in the paraffin-embedded IUGR villi could ultimately contribute to an aberrant nutrient–gas exchange at the IUGR maternal-fetal membrane. These results demonstrate that IUGR CT can still mediate cell fusions (index of 63.24%) despite greatly reduced amounts of fusogenic Syncytin-1 and -2. It is important to note that Syncytin-3 concentrations remained unchanged between control and IUGR placentae and CT and therefore seem not to play a role in the molecular etiology of IUGR. In addition to fusogenic Syncytins and their receptors, several other mechanisms and proteins have been proposed to be involved in CT fusion like (1) a phosphatidyl serine flip [46], (2) connexin 43 [47], (3) cadherin 11 [48], (4) CD98 and the ligand galectin 3 [49], and (5) caspase 8, which plays a role in a small time window just shortly before cell fusion [50, 51].

The regulatory mechanisms of Syncytin-1 and -2 gene expression are still under investigation. Many regulatory elements critical for the transcriptional regulation have been

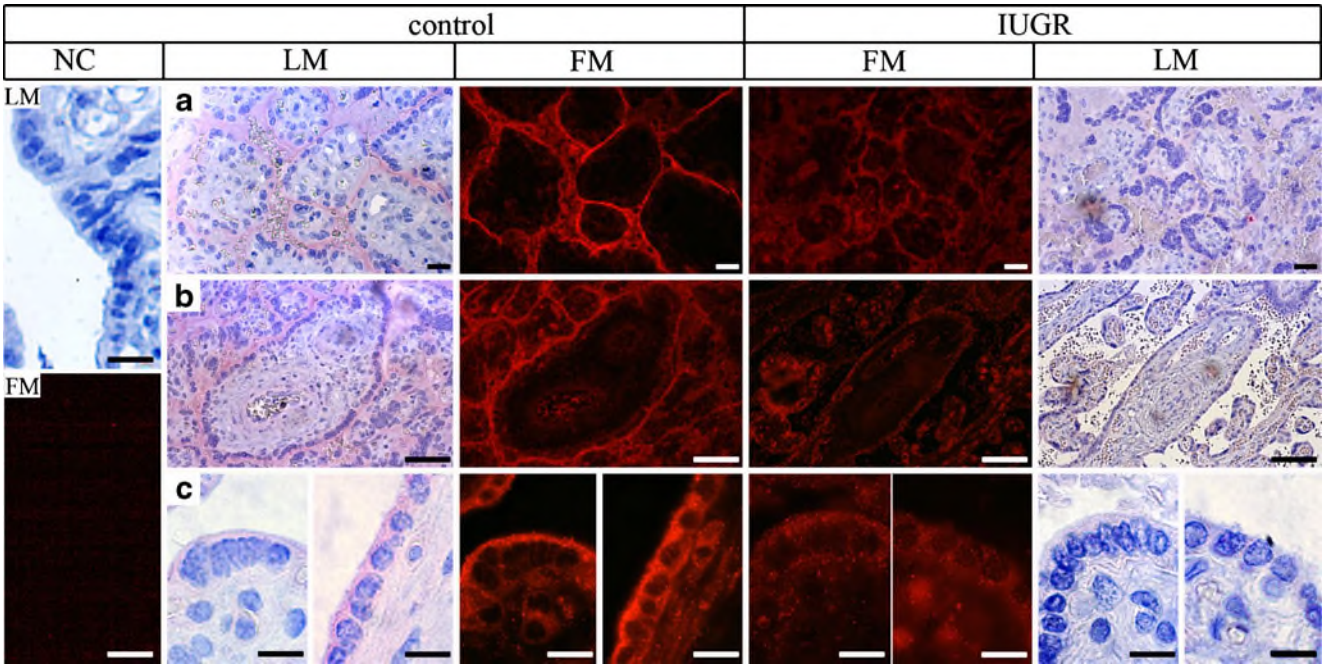

Fig. 5 a–c Paraffin-embedded placentae from control and IUGR patients were deparaffinized and incubated with Syncytin-1 polyclonal antibody against the SU-domain, stained with Fast Red–Hematoxylin, and visualized with light microscopy (*LM*) and fluorescence microscopy (*FM*) at 670 nm. Note the decreased Syncytin-1 protein signal in IUGR tissue. *Bars* represent 50 (*A*, *B*) and 100 μm (*C*). Negative control (*NC*) for Fast Red staining was performed in the absence of the primary (Syncytin-1) antibody

proposed for HERV-W, e.g., the CCAAT motif and the octamer protein binding site of the promoter region in the 5′-long terminal repeat (LTR) [52]. Upstream of the 5′LTR are binding sites for the transcription factor Glia Cell Missing a (GCMa) which enhances Syncytin-1 expression as demonstrated in the choriocarcinoma cell lines BeWo and JEG-3 [53]. Recently, an estrogen response element was identified in the 5′LTR of HERV-W, which was important for the upregulation of Syncytin-1 after estradiol treatment [23]. On the other hand, mutations of the ecdysone receptor response element enhance the basal promoter activity, which could be a silencer for Syncytin-1 transcription [52]. It has also been demonstrated that Syncytin-1 transcription was regulated by CpG-methylation in the 5′ LTR of HERV-W [54]. Therefore, it is possible that in IUGR placentae, hypermethylation of CpGs in the LTR of HERV-W could reduce Syncytin-1 expression, a regulation which could also involve other HERV genes (Ruebner et al., manuscript in preparation). Hypoxia is also a known regulator of Syncytin-1 expression and β-hCG secretion [20]. In this report we determined that cultured control and IUGR CT at ~20% oxygen showed differences in HERV env gene expression levels and which were also comparable to levels in their respective primary placentae (controls and IUGR).

In addition to the three fusogenic Syncytins, the env genes of HERV-R (envERV3), HERV-V1, and -V2 were analyzed in placentae and isolated CT. EnvERV3 presented the second highest expression level in control placentae and control CT. Although we found that envERV3 expression levels remained similar between control and IUGR placentae, a significantly lower expression was detected in IUGR CT compared to control CT following a 3-day cultivation period (7.5-fold lower, $P=0.020921$; Table 2). This difference in expression could be explained by the fact that envERV3 was not detected in isolated normal undifferentiated CT, but highly expressed in SCT after cultivation, thus showing cell type specificity [55, 56]. Therefore, reduced envERV3 expression is linked with aberrant cell fusion capabilities of IUGR CT to SCT. On the other hand, the similar envERV3 expression between control and IUGR placenta tissues could be due to other cell types than CT, which contribute to envERV3 expression. Although, envERV3 is not considered a fusogenic env gene by ex vivo studies, in the choriocarcinoma cell line BeWo, Forskolin treatment upregulated envERV3 in conjunction with β-hCG and cell fusion [57]. EnvERV3 transfections led to increased cAMP levels which in turn also upregulated β-hCG [58, 59]. In addition, transfected envERV3 had an effect on the cell cycle regulators cyclin B and p21 causing growth inhibition. Taken together, envERV3 was proposed necessary for the final differentiation process of CT cell fusion to SCT [57]. Therefore, it is possible that downregulation of envERV3 like Syncytin-1 could contribute to IUGR, esp. linked with a reduction of both β-hCG and cell fusion.

Although envV1 and envV2 were significantly expressed lower in IUGR compared to control placentae, both env genes were highly upregulated in isolated CT from control placentae, placing them to the third and fourth highest after Syncytin-1 and envERV3. EnvV1 and envV2 were exclusively detected in placentae; they were not fusogenic by in vitro assays [28]. Considering the preservation of envV1 and envV2 in evolution, envV2 was shown conserved in all simians, whereas envV1 was intact in chimpanzee and rhesus macaque [33], and in view of the high expression of envV1 and envV2 in cultivated CT, a beneficial role for placentogenesis similar to Syncytin-1 and -2 can be proposed.

HCG is a glycoprotein hormone comprising two subunits, an alpha and a beta joined noncovalently. However, different hCG species exist, e.g., intact hCG, α-hCG, β-hCG, hyperglycosylated hCG, nicked hCG, and β-hCG fragments. While hCG is made by the SCT, hyperglycosylated hCG is made by extravillous CT, and all have been analyzed in the literature with different antibodies [60, 61]. It is known that elevated serum hCG levels were noted in the first and second trimester of IUGR [62, 63]. For example, Lepage et al. [63] found high maternal hCG in ~22% second-trimester pregnancies with complications, like spontaneous miscarriage, hypertensive disorder, or SGA, but also in ~11% of control pregnancies. In addition, some SGA/IUGR infants were complicated with Down syndrome, which resulted in extremely high hCG levels. In contrast, none of the analyzed placentas in our study had other obstetric complications than IUGR and no Down syndrome. A previous study about IUGR and β-hCG levels in the third trimester unraveled that additional factors could play a role [64]. For example, toxemia resulted in elevated levels of hCG, whereas IUGR without toxemia had normal β-hCG levels. In contrast to our present results and Langbein et al. [35], Newhouse et al. [65] found higher syncytialization and β-hCG secretion of IUGR CT compared to control CT. The IUGR cohort of Newhouse et al. [65] mostly consisted of patients with normal Doppler (66%), whereas our IUGR cohort had exclusively abnormal Doppler, in line with different IUGR clinical groups according to Mandruzzato et al. [34]. Interestingly, the lower syncytialization and β-hCG expression of the PE/IUGR cohort from Newhouse et al. [65] was similar to Langbein et al. [35]. In summary, we propose that different types and levels of hCG has to be more specified and warrant comparing similar clinical sub-groups of IUGR along with other obstetric complications. Thus, in particular, β-hCG levels could represent a marker for IUGR severity.

Lastly, regarding ASCT-1 and -2, the two putative receptors of Syncytin-1, no significant differences in expression between control and IUGR placentae were found. The expression analysis of placentae from patients with pre-eclampsia also showed no alteration for ASCT-2 [17]. In contrast to the placental tissues, a significant upregulation of ASCT-1 and -2 expressions was found in cultivated IUGR CT compared to control CT (Table 3). The increase of the receptor expression in isolated IUGR CT could point to a compensation for the lower Syncytin-1 expression. Glucose is transported by the two main families GLUT (facilitated diffusion glucose transporters) and SGLT (sodium-dependent glucose transporters), where the transporter GLUT-1 was found not reduced in IUGR SCT [66]. On the other hand, increased or decreased glucose consumption has been discussed regarding IUGR placentae, as well as an altered glycolytic pathway [67]. Interestingly, we determined a significant 1.5-fold reduced serum glucose concentration in IUGR compared to control newborns (Table 1). In addition, the placenta-specific receptor for Syncytin-2 MFSD2 was significantly downregulated in IUGR placentae and CT (Table 3). MFSD2 is a putative placental carbohydrate transporter, and the significant downregulation found in IUGR placentae and CT could be responsible for the significant lower glucose content in the newborn IUGR children (Table 3). In conclusion, understanding the developmental process of placentogenesis, esp. the role of HERV env in fusion and other aspects, will be important for unraveling pathological processes of the placenta.

Acknowledgments The authors are especially grateful to the patients who participated in this study and to the Dept. of Gynaecology and Obstetrics, Erlangen. The authors thank Dr. Kristina Becker (Inst. for Biochemistry, University of Erlangen-Nuremberg) and Florentine Koppitz and Elisabeth Stiegler (Dept. of Gynaecology and Obstetrics, Erlangen) for expert technical assistance. This work was supported by a grant from the "Deutsche Forschungsgemeinschaft" (DFG) to RS.

References

1. Potgens AJ, Schmitz U, Bose P, Versmold A, Kaufmann P, Frank HG (2002) Mechanisms of syncytial fusion: a review. Placenta 23 (Suppl A):S107–S113. doi:10.1053/plac.2002.0772
2. Watson AL, Skepper JN, Jauniaux E, Burton GJ (1998) Changes in concentration, localization and activity of catalase within the human placenta during early gestation. Placenta 19:27–34
3. Jauniaux E, Poston L, Burton GJ (2006) Placental-related diseases of pregnancy: Involvement of oxidative stress and implications in human evolution. Hum Reprod Update 12:747–755. doi:10.1093/humupd/dml016
4. Getzowa S, Sadowsky A (1950) On the structure of the human placenta with full-time and immature foetus, living or dead. J Obstet Gynaecol Br Emp 57:388–396
5. Cetin I, Foidart JM, Miozzo M, Raun T, Jansson T, Tsatsaris V, Reik W, Cross J, Hauguel-de-Mouzon S, Illsley N, Kingdom J, Huppertz B (2004) Fetal growth restriction: a workshop report. Placenta 25:753–757. doi:10.1016/j.placenta.2004.02.004

6. Pollack RN, Divon MY (1992) Intrauterine growth retardation: definition, classification, and etiology. Clin Obstet Gynecol 35:99–107
7. Maulik D, Frances Evans J, Ragolia L (2006) Fetal growth restriction: pathogenic mechanisms. Clin Obstet Gynecol 49:219–227
8. Wallner W, Sengenberger R, Strick R, Strissel PL, Meurer B, Beckmann MW, Schlembach D (2007) Angiogenic growth factors in maternal and fetal serum in pregnancies complicated by intrauterine growth restriction. Clin Sci (Lond) 112:51–57. doi:10.1042/CS20060161
9. Biswas S, Ghosh SK, Chhabra S (2008) Surface area of chorionic villi of placentas: an index of intrauterine growth restriction of fetuses. J Obstet Gynaecol Res 34:487–493. doi:10.1111/j.1447-0756.2008.00719.x
10. Huppertz B, Kadyrov M, Kingdom JC (2006) Apoptosis and its role in the trophoblast. Am J Obstet Gynecol 195:29–39. doi:10.1016/j.ajog.2005.07.039
11. Ishihara N, Matsuo H, Murakoshi H, Laoag-Fernandez JB, Samoto T, Maruo T (2002) Increased apoptosis in the syncytiotrophoblast in human term placentas complicated by either preeclampsia or intrauterine growth retardation. Am J Obstet Gynecol 186:158–166
12. Jurka J (2000) Repbase update: a database and an electronic journal of repetitive elements. Trends Genet 16:418–420
13. Villesen P, Aagaard L, Wiuf C, Pedersen FS (2004) Identification of endogenous retroviral reading frames in the human genome. Retrovirology 1:32. doi:10.1186/1742-4690-1-32
14. Cheynet V, Ruggieri A, Oriol G, Blond JL, Boson B, Vachot L, Verrier B, Cosset FL, Mallet F (2005) Synthesis, assembly, and processing of the Env ERVWE1/syncytin human endogenous retroviral envelope. J Virol 79:5585–5593. doi:10.1128/JVI.79.9.5585-5593.2005
15. Mallet F, Bouton O, Prudhomme S, Cheynet V, Oriol G, Bonnaud B, Lucotte G, Duret L, Mandrand B (2004) The endogenous retroviral locus ERVWE1 is a bona fide gene involved in hominoid placental physiology. Proc Natl Acad Sci USA 101:1731–1736. doi:10.1073/pnas.0305763101 0305763101
16. Kingdom FA, Keeble DR (2000) Luminance spatial frequency differences facilitate the segmentation of superimposed textures. Vis Res 40:1077–1087
17. Chen CP, Wang KG, Chen CY, Yu C, Chuang HC, Chen H (2006) Altered placental syncytin and its receptor ASCT2 expression in placental development and pre-eclampsia. BJOG 113:152–158. doi:10.1111/j.1471-0528.2005.00843.x
18. Heazell AE, Buttle HR, Baker PN, Crocker IP (2008) Altered expression of regulators of caspase activity within trophoblast of normal pregnancies and pregnancies complicated by preeclampsia. Reprod Sci 15:1034–1043. doi:10.1177/1933719108322438 15/10/1034
19. Cetin I, Alvino G (2009) Intrauterine growth restriction: implications for placental metabolism and transport. A review. Placenta 30(Suppl A):S77–S82. doi:10.1016/j.placenta.2008.12.006
20. Wich C, Kausler S, Dotsch J, Rascher W, Knerr I (2009) Syncytin-1 and glial cells missing a: hypoxia-induced deregulated gene expression along with disordered cell fusion in primary term human trophoblasts. Gynecol Obstet Invest 68:9–18. doi:10.1159/000209396
21. Marin M, Lavillette D, Kelly SM, Kabat D (2003) N-linked glycosylation and sequence changes in a critical negative control region of the ASCT1 and ASCT2 neutral amino acid transporters determine their retroviral receptor functions. J Virol 77:2936–2945
22. Bjerregaard B, Holck S, Christensen IJ, Larsson LI (2006) Syncytin is involved in breast cancer-endothelial cell fusions. Cell Mol Life Sci 63:1906–1911. doi:10.1007/s00018-006-6201-9
23. Strick R, Ackermann S, Langbein M, Swiatek J, Schubert SW, Hashemolhosseini S, Koscheck T, Fasching PA, Schild RL, Beckmann MW, Strissel PL (2007) Proliferation and cell–cell fusion of endometrial carcinoma are induced by the human endogenous retroviral Syncytin-1 and regulated by TGF-beta. J Mol Med 85:23–38. doi:10.1007/s00109-006-0104-y
24. Pawelek JM, Chakraborty AK (2008) Fusion of tumour cells with bone marrow-derived cells: a unifying explanation for metastasis. Nat Rev Cancer 8:377–386. doi:10.1038/nrc2371
25. Blaise S, de Parseval N, Benit L, Heidmann T (2003) Genome-wide screening for fusogenic human endogenous retrovirus envelopes identifies syncytin 2, a gene conserved on primate evolution. Proc Natl Acad Sci USA 100:13013–13018. doi:10.1073/pnas.2132646100
26. Malassine A, Blaise S, Handschuh K, Lalucque H, Dupressoir A, Evain-Brion D, Heidmann T (2007) Expression of the fusogenic HERV-FRD Env glycoprotein (syncytin 2) in human placenta is restricted to villous cytotrophoblastic cells. Placenta 28:185–191. doi:10.1016/j.placenta.2006.03.001
27. Esnault C, Priet S, Ribet D, Vernochet C, Bruls T, Lavialle C, Weissenbach J, Heidmann T (2008) A placenta-specific receptor for the fusogenic, endogenous retrovirus-derived, human syncytin-2. Proc Natl Acad Sci USA 105:17532–17537. doi:10.1073/pnas.0807413105
28. Blaise S, de Parseval N, Heidmann T (2005) Functional characterization of two newly identified Human Endogenous Retrovirus coding envelope genes. Retrovirology 2:19. doi:10.1186/1742-4690-2-19
29. Kato N, Pfeifer-Ohlsson S, Kato M, Larsson E, Rydnert J, Ohlsson R, Cohen M (1987) Tissue-specific expression of human provirus ERV3 mRNA in human placenta: two of the three ERV3 mRNAs contain human cellular sequences. J Virol 61:2182–2191
30. Cohen M, Kato N, Larsson E (1988) ERV3 human endogenous provirus mRNAs are expressed in normal and malignant tissues and cells, but not in choriocarcinoma tumor cells. J Cell Biochem 36:121–128. doi:10.1002/jcb.240360203
31. de Parseval N, Heidmann T (1998) Physiological knockout of the envelope gene of the single-copy ERV-3 human endogenous retrovirus in a fraction of the Caucasian population. J Virol 72:3442–3445
32. Herve CA, Forrest G, Lower R, Griffiths DJ, Venables PJ (2004) Conservation and loss of the ERV3 open reading frame in primates. Genomics 83:940–943. doi:10.1016/j.ygeno.2003.10.003
33. Kjeldbjerg AL, Villesen P, Aagaard L, Pedersen FS (2008) Gene conversion and purifying selection of a placenta-specific ERV-V envelope gene during simian evolution. BMC Evol Biol 8:266. doi:10.1186/1471-2148-8-266
34. Mandruzzato G, Antsaklis A, Botet F, Chervenak FA, Figueras F, Grunebaum A, Puerto B, Skupski D, Stanojevic M (2008) Intrauterine restriction (IUGR). J Perinat Med 36:277–281. doi:10.1515/JPM.2008.050
35. Langbein M, Strick R, Strissel PL, Vogt N, Parsch H, Beckmann MW, Schild RL (2008) Impaired cytotrophoblast cell–cell fusion is associated with reduced Syncytin and increased apoptosis in patients with placental dysfunction. Mol Reprod Dev 75:175–183. doi:10.1002/mrd.20729
36. Kliman HJ, Nestler JE, Sermasi E, Sanger JM, Strauss JF 3rd (1986) Purification, characterization, and in vitro differentiation of cytotrophoblasts from human term placentae. Endocrinology 118:1567–1582
37. Newby D, Dalgliesh GL, Aitken DA, Lyall F (2007) Effect of cryopreservation on human cytotrophoblast cells in culture: hCG and PALP production. Placenta 28:350–352. doi:10.1016/j.placenta.2006.04.012
38. Guilbert LJ, Winkler-Lowen B (2007) Placental alkaline phosphatase (PLAP) staining and human chorionic gonadotropin

(hCG) production in cultures of fresh and cryopreserved cytotrophoblasts isolated by CD9/MHC class I/MHC class II immunoelimination. Placenta 28:348–349. doi:10.1016/j.placenta.2006.04.011
39. Frendo JL, Vidaud M, Guibourdenche J, Luton D, Muller F, Bellet D, Giovagrandi Y, Tarrade A, Porquet D, Blot P, Evain-Brion D (2000) Defect of villous cytotrophoblast differentiation into syncytiotrophoblast in Down's syndrome. J Clin Endocrinol Metab 85:3700–3707
40. Handschuh K, Guibourdenche J, Cocquebert M, Tsatsaris V, Vidaud M, Evain-Brion D, Fournier T (2009) Expression and regulation by PPARgamma of hCG alpha- and beta-subunits: comparison between villous and invasive extravillous trophoblastic cells. Placenta 30:1016–1022. doi:10.1016/j.placenta.2009.09.006
41. Vargas A, Moreau J, Landry S, LeBellego F, Toufaily C, Rassart E, Lafond J, Barbeau B (2009) Syncytin-2 plays an important role in the fusion of human trophoblast cells. J Mol Biol 392:301–318. doi:10.1016/j.jmb.2009.07.025
42. de Parseval N, Lazar V, Casella JF, Benit L, Heidmann T (2003) Survey of human genes of retroviral origin: identification and transcriptome of the genes with coding capacity for complete envelope proteins. J Virol 77:10414–10422
43. Blond JL, Lavillette D, Cheynet V, Bouton O, Oriol G, Chapel-Fernandes S, Mandrand B, Mallet F, Cosset FL (2000) An envelope glycoprotein of the human endogenous retrovirus HERV-W is expressed in the human placenta and fuses cells expressing the type D mammalian retrovirus receptor. J Virol 74:3321–3329
44. Frendo JL, Olivier D, Cheynet V, Blond JL, Bouton O, Vidaud M, Rabreau M, Evain-Brion D, Mallet F (2003) Direct involvement of HERV-W Env glycoprotein in human trophoblast cell fusion and differentiation. Mol Cell Biol 23:3566–3574
45. Knerr I, Beinder E, Rascher W (2002) Syncytin, a novel human endogenous retroviral gene in human placenta: evidence for its dysregulation in preeclampsia and HELLP syndrome. Am J Obstet Gynecol 186:210–213
46. Adler RR, Ng AK, Rote NS (1995) Monoclonal antiphosphatidylserine antibody inhibits intercellular fusion of the choriocarcinoma line, JAR. Biol Reprod 53:905–910
47. Cronier L, Guibourdenche J, Niger C, Malassine A (1999) Oestradiol stimulates morphological and functional differentiation of human villous cytotrophoblast. Placenta 20:669–676. doi:10.1053/plac.1999.0423
48. Getsios S, MacCalman CD (2003) Cadherin-11 modulates the terminal differentiation and fusion of human trophoblastic cells in vitro. Dev Biol 257:41–54
49. Dalton P, Christian HC, Redman CW, Sargent IL, Boyd CA (2007) Membrane trafficking of CD98 and its ligand galectin 3 in BeWo cells—implication for placental cell fusion. FEBS J 274:2715–2727. doi:10.1111/j.1742-4658.2007.05806.x
50. Gauster M, Moser G, Orendi K, Huppertz B (2009) Factors involved in regulating trophoblast fusion: potential role in the development of preeclampsia. Placenta 30(Suppl A):S49–S54. doi:10.1016/j.placenta.2008.10.011
51. Gauster M, Siwetz M, Huppertz B (2009) Fusion of villous trophoblast can be visualized by localizing active caspase 8. Placenta 30:547–550. doi:10.1016/j.placenta.2009.03.007
52. Cheng YH, Richardson BD, Hubert MA, Handwerger S (2004) Isolation and characterization of the human syncytin gene promoter. Biol Reprod 70:694–701. doi:10.1095/biolreprod.103.023473
53. Yu C, Shen K, Lin M, Chen P, Lin C, Chang GD, Chen H (2002) GCMa regulates the syncytin-mediated trophoblastic fusion. J Biol Chem 277:50062–50068. doi:10.1074/jbc.M209316200
54. Matouskova M, Blazkova J, Pajer P, Pavlicek A, Hejnar J (2006) CpG methylation suppresses transcriptional activity of human syncytin-1 in non-placental tissues. Exp Cell Res 312:1011–1020. doi:10.1016/j.yexcr.2005.12.010
55. Boyd MT, Bax CM, Bax BE, Bloxam DL, Weiss RA (1993) The human endogenous retrovirus ERV-3 is upregulated in differentiating placental trophoblast cells. Virology 196:905–909. doi:10.1006/viro.1993.1556
56. Venables PJ, Brookes SM, Griffiths D, Weiss RA, Boyd MT (1995) Abundance of an endogenous retroviral envelope protein in placental trophoblasts suggests a biological function. Virology 211:589–592. doi:10.1006/viro.1995.1442
57. Lin L, Xu B, Rote NS (1999) Expression of endogenous retrovirus ERV-3 induces differentiation in BeWo, a choriocarcinoma model of human placental trophoblast. Placenta 20:109–118. doi:10.1053/plac.1998.0337
58. Lin L, Xu B, Rote NS (2000) The cellular mechanism by which the human endogenous retrovirus ERV-3 env gene affects proliferation and differentiation in a human placental trophoblast model, BeWo. Placenta 21:73–78. doi:10.1053/plac.1999.0443
59. Prudhomme S, Oriol G, Mallet F (2004) A retroviral promoter and a cellular enhancer define a bipartite element which controls env ERVWE1 placental expression. J Virol 78:12157–12168. doi:10.1128/JVI.78.22.12157-12168.2004
60. Cole LA (2009) New discoveries on the biology and detection of human chorionic gonadotropin. Reprod Biol Endocrinol 7:8. doi:10.1186/1477-7827-7-8
61. de Medeiros SF, Norman RJ (2009) Human choriogonadotrophin protein core and sugar branches heterogeneity: basic and clinical insights. Hum Reprod Update 15:69–95. doi:10.1093/humupd/dmn036
62. Odibo AO, Sehdev HM, Stamilio DM, Macones GA (2006) Evaluating the thresholds of abnormal second trimester multiple marker screening tests associated with intra-uterine growth restriction. Am J Perinatol 23:363–367. doi:10.1055/s-2006-947724
63. Lepage N, Chitayat D, Kingdom J, Huang T (2003) Association between second-trimester isolated high maternal serum maternal serum human chorionic gonadotropin levels and obstetric complications in singleton and twin pregnancies. Am J Obstet Gynecol 188:1354–1359
64. Heikinheimo M, Seppala M (1983) Amniotic fluid human chorionic gonadotropin in late pregnancy: elevated levels in toxemia with intrauterine growth retardation. Am J Obstet Gynecol 146:766–768
65. Newhouse SM, Davidge ST, Winkler-Lowen B, Demianczuk N, Guilbert LJ (2007) In vitro differentiation of villous trophoblasts from pregnancies complicated by intrauterine growth restriction with and without pre-eclampsia. Placenta 28:999–1003. doi:10.1016/j.placenta.2007.04.008
66. Jansson T, Ylven K, Wennergren M, Powell TL (2002) Glucose transport and system A activity in syncytiotrophoblast microvillous and basal plasma membranes in intrauterine growth restriction. Placenta 23:392–399. doi:10.1053/plac.2002.0826
67. Magnusson AL, Powell T, Wennergren M, Jansson T (2004) Glucose metabolism in the human preterm and term placenta of IUGR fetuses. Placenta 25:337–346. doi:10.1016/j.placenta.2003.08.021